

## pH- and Voltage-dependent Conductances in Toad Skin

F. Lacaz-Vieira

Department of Physiology and Biophysics, Institute of Biomedical Sciences, University of São Paulo, 05508-900 São Paulo, Brazil

Received: 24 April 1995/Revised: 6 July 1995

**Abstract.** The present study focuses on two closely related topics on ion conductance in toad skins: (i) the interaction of apical protons with the apical voltage-dependent  $\text{Cl}^-$ -activated channels of the mitochondria-rich cells, and (ii) the description and characterization of a novel subject, a voltage-dependent  $\text{H}^+$ -activated conductance.

The  $\text{Cl}^-$  conductance ( $G_{\text{Cl}}$ ) is activated by tissue hyperpolarization (which leads to apical membrane depolarization) and the presence of  $\text{Cl}^-$  ions in the apical solution. Increasing apical proton concentration (from pH 8 to pH 4) impairs the process of activation of the  $\text{Cl}^-$  conductive pathway, slowing the kinetics of  $I_t$  activation and reducing the steady-state values of  $G_t$  and  $I_r$ . This effect is markedly voltage-dependent since no effect is seen at  $V_t = -100$  mV and is fully present at  $-50$  mV. The voltage-dependence of the pH effect suggests that the critical protonation sites of the apical  $\text{Cl}^-$  channels are not freely exposed to the apical solution but dwell within the membrane electric field. An also coherent interpretation is that titration of apical proton binding sites affects the gating of the voltage-dependent  $\text{Cl}^-$  channels, shifting the conductance-vs.-voltage curve to more negative clamping potentials.

Tissue conductance in the absence of apical  $\text{Cl}^-$  ions can be importantly affected by the pH of the apical solution ( $\text{pH}_a$ ), the effect being markedly dependent on the clamping potential. Generally speaking, the effect of rising apical proton concentration can be conspicuous at negative clamping potentials, while at positive potentials changes in tissue conductance were never observed. For a clamping potential of  $-100$  mV, a turning point somewhere between  $\text{pH}_a = 4$  and  $\text{pH}_a = 3$  was observed. Apical acidification to pH 4 has no effect upon tissue conductance while apical acidification to pH 3 leads to a

marked, slow and reversible increase of tissue conductance. A striking similitude exists between the voltage-dependent  $\text{Cl}^-$ -gated conductance and the voltage-dependent proton-gated conductance regarding: (i) slow time courses of activation and deactivation, (ii) requirement for a negative clamping potential and the presence of a specific ion species in the apical solution for activation to take place, (iv) instantaneous ohmic behavior, and (v) steady-state rectification. However, so far the results do not permit one to conclude definitely that the voltage-dependent  $\text{Cl}^-$ -gated conductance and the voltage-dependent proton-gated conductance share a common pathway.

**Key words:** Toad skin — pH — Ion conductance — Voltage dependence — Chloride conductance

### Introduction

Epithelia have, among other functions, the ability to absorb or to secrete fluid.  $\text{Cl}^-$  channels play, among different functions, a key role in  $\text{Cl}^-$  absorbing or secreting epithelia, in cellular volume regulation, and in stabilization of membrane potential (Gogelein, 1989; Pusch & Jentsch, 1994). The chloride conductance ( $G_{\text{Cl}}$ ) in amphibian skins has been associated with a voltage-dependent pathway (Bruus, Kristensen & Larsen, 1976; Larsen & Kristensen, 1978; Larsen, 1982; Larsen & Rasmussen, 1982, 1983, 1985; Lacaz-Vieira & Procopio, 1988a,b; Procopio & Lacaz-Vieira, 1990). Chloride channels presumed to be located in the apical membrane of the mitochondria-rich cells apparently are implicated in this process (Foskett & Ussing, 1986; Spring & Ussing, 1986; Larsen, Ussing & Spring, 1987; Larsen & Harvey, 1994). Activation of  $G_{\text{Cl}}$  results from depolarization of the apical membrane in response to whole tissue hyperpolarization and is critically dependent on the presence of  $\text{Cl}^-$  in the apical solution. In its absence,

conductance activation does not take place even when the apical membrane is depolarized (Kristensen & Larsen, 1978; Hareck & Larsen, 1986). In short-circuited tissues,  $G_{Cl}$  activation is induced by apical exposure to  $Cl^-$  or  $Br^-$ , whereas  $I^-$ ,  $SCN^-$ , gluconate, and  $SO_4^{2-}$  are without effect. Once activated, the conductive pathway exhibit a poor anion selectivity indicating that it can be more properly referred to as an anion-permeable pathway than a specific  $Cl^-$  pathway (Larsen, 1991). So far, the available data indicate that regulation occurs at a  $Cl^-$  (or  $Br^-$ ) ion-specific site remote from a poor anion-selective translocation site of the channel (Kristensen, 1982).

Besides being controlled by the potential difference and the apical  $Cl^-$  or  $Br^-$  concentration, the anion conductive pathway also seems to be modulated by a c-AMP-dependent process (Cuthbert & Painter, 1968; Mandel, 1975; Kristensen, 1983; Katz & Larsen, 1984; Katz & Van Driessche, 1987), c-AMP shifting the  $G_i$ -vs.- $V$  curve along the  $V$  axis (Willumsen, Vestergaard & Larsen, 1992). The observation of a Lorentzian component in the power density spectrum of forskolin-treated frog skins that depends on the presence of  $Cl^-$  in the bathing solutions and are modified by  $Cl^-$  channel blockers also support the existence of c-AMP-activated  $Cl^-$  channels in frog skin (De Wolf, Van Driessche & Nagel, 1989).

Ion channels of plasma membrane of neurons (Hille, 1968; Tang, Dichter & Morad, 1990; Ueno, Nakaye & Akaïke, 1992), muscles (Pietrobon, Prod'hom & Hess, 1989; Prod'hom, Pietrobon & Hess, 1989), epithelial cells (Kuwahara et al., 1989; Chang, Kushman & Dawson, 1991; Klaerke et al., 1993; Suzuki et al., 1994), lymphocytes (Deutsch & Lee, 1989) organelles (Rousseau & Pinkos, 1990), and others (Wilmsen, Pugsley & Pattus, 1990; Todt & McGroarty, 1992; Todt, Rocque & McGroarty, 1992) are affected by the concentration of protons in the bathing solutions. These effects may result from changes of the kinetics of activation or inactivation, single-channel conduction, or ionic selectivity. Ion-conducting channels formed in lipid bilayers by diphtheria toxin are highly pH dependent, the channel's single-channel conductance and selectivity depending on proton concentration on either side of the membrane (Mindell et al., 1994a,b). The study of mutant channels unveiled an important aspect that a few charged residues, sometimes a single residue, is responsible for the pH effect (Mindell et al., 1994a,b).  $Cl^-$  channels in different structures are affected by the proton concentration in the bathing solutions. In colonic epithelial cells intracellular pH regulates  $G_{Cl}$  by modulating  $Ca^{2+}$  activation, external pH having no effect (Chang, Kushman & Dawson, 1991).  $Cl^-$ -channels of the gastric parietal cell incorporated into lipid bilayers are active at low pH on the *trans* side, a low  $pH_{trans}$ , increasing channel open probability, but reduction of the pH on the *cis* side from 7.4 to 3

always resulted in loss of channel activity (Cuppoletti, Baker & Malinowska, 1993). A differential acidic pH sensitivity between normal and delta F508 CFTR  $Cl^-$ -channel activity in lipid bilayers has been reported and may be of significance to the understanding the cystic fibrosis defect since normal CFTR can function in the environment of acidic intracellular organelles, whereas the activity of mutant CFTR would be greatly reduced (Sherry, Cuppoletti & Malinowska, 1994).

The existence of a voltage sensor (charges or dipoles that move under the influence of the membrane electric field) is essential for the mechanism of voltage dependence of ion channels. Surface charges on ion channel proteins may affect their function in several ways (for review *see* (Green & Andersen, 1991; Latorre, Labarca & Naranjo, 1992; Jordan, 1993). They may influence conductance by changing the concentration of permeant counter-ions according to a Boltzmann distribution (MacInnes, 1961; Apell, Bamberg & Läuger, 1979; Hille, 1992), modulating gating kinetics (Behrens et al., 1989) or influencing transitions to subconductance states (Recio-Pinto et al., 1990). Thus, it can be expected that the function of ion channels might be modulated, among other variables, by the degree of protonation of the membrane surface charges which are highly affected by the concentration of hydrogen ions in the solutions bathing the membrane in which the channels are incorporated.

## Materials and methods

### PREPARATION

Abdominal skins of double-pithed toad *Bufo marinus* were used. A plastic ring of 20 mm diameter was glued to the apical surface of the skin with ethylcyanoacrylate adhesive (Super Bonder, Loctite Brasil Ltda). The fragment of tissue framed by the plastic ring was excised, immersed in Ringer solution and subsequently mounted in a modified Ussing's chamber (Castro, Sesso & Lacaz-Vieira, 1993), exposing an area of 0.5 cm<sup>2</sup>. Hemichambers with a recessed rim filled with high viscosity silicone grease (Dow Corning High Vacuum Grease) prevented tissue edge damage (Lacaz-Vieira, 1986). Each chamber compartment was perfused with a continuous flow of solution (up to 25 ml/min) driven by gravity. Unstirred layers on the tissue surfaces were minimized by directing the incoming fluid towards the surfaces of the tissue. Each compartment was drained through a spillway open to the atmosphere, so that the pressure inside each compartment was kept constant at the atmospheric level. Rapid solution changes were obtained, without interrupting the voltage clamping, by switching the inlet tubings at their connections with the chamber.

### ELECTRICAL MEASUREMENTS

A conventional analogue voltage clamp (WPI DVC 1000) was used. Saturated calomel half-cells with 3 M KCl-agar bridges were used to measure the electrical potential difference across the skin. Current was passed through Ag-AgCl 3 M KCl electrodes and 3 M KCl-agar bridges, adequately placed to deliver a uniform current density across the skin.

The clamping current was continuously recorded by a strip-chart recorder. Clamping current and voltage were also digitized through an analog-to-digital converter (Digidata 1200 and Axotape 2.0, Axon Instruments) and recorded in a computer (Microtec 386 SX) for further processing. Current-voltage relationships were obtained by applying voltage steps, generated by a computer driven digital-to-analog converter connected to the external command port of the voltage clamp in order to impose clamping potentials of  $-200, 200, -180, 180, -160, 160, \dots, -20, 20,$  and  $0$  mV, of 100 msec duration or less, on top of the previous holding potential.

## SOLUTIONS

The inner bathing solution was NaCl Ringer in all experiments, with the following composition (in mM): NaCl 115,  $\text{KHCO}_3$  2.5, and  $\text{CaCl}_2$  1.0, with a pH of 8.2 after aeration. The apical bathing fluids were simple salt solutions, nonbuffered, without added  $\text{Ca}^{++}$  prepared with glass distilled water, having pH around 6.0 and free- $\text{Ca}^{2+}$  concentration in the range of  $1.5 \times 10^{-7}$  and  $2.0 \times 10^{-7}$  M (Castro et al., 1993). Apical solution pHs were adjusted by adding HCl or  $\text{H}_2\text{SO}_4$  (according to the main anion present in the apical solution) or KOH.

## STATISTICS

The results are presented as mean  $\pm$  SEM. Comparisons were carried out using Student's paired *t*-test. When more than two groups were compared, significance was determined by two-way analysis of variance followed by appropriate post-test comparison. The *P* values cited include Bonferroni's correction (Neter & Wasserman, 1974).

## ABBREVIATIONS

$G_t$ , Total transmembrane electrical conductance, in  $\text{mS}/\text{cm}^2$ . Calculated from the deflections of the clamping current induced by shifts of the clamping potential of 300 msec duration,  $\pm 10$  mV amplitude at 15-sec intervals, as  $G_t = \Delta I_t / \Delta V_p$ , where  $\Delta V_p$  and  $\Delta I_t$  are the changes in the electrical potential difference across the tissue and clamping current, respectively.  $I_t$ , Clamping-current, in  $\mu\text{A}/\text{cm}^2$ . Positive (or inward) current corresponds to the transport of positive charges across the tissue, from the apical to the inner bathing solution.  $V_t$ , Electrical potential difference across the tissue, in mV. The potential of the apical solution is referred to that of the inner solution.  $\text{pH}_a$ , pH of the apical solution.  $[\text{Cl}^-]_a$ ,  $\text{Cl}^-$  concentration in the apical solution.

## Results

### EFFECTS OF APICAL pH AND CLAMPING POTENTIAL ON THE ACTIVATION OF THE $\text{Cl}^-$ CONDUCTIVE PATHWAY

The present experiments aimed to evaluate the effects of  $\text{pH}_a$  on the activation of the voltage-dependent  $\text{Cl}^-$ -gated  $G_{\text{Cl}}$ . The results show a marked interdependence of  $\text{pH}_a$  and clamping potential ( $V_t$ ) on the activation of the  $\text{Cl}^-$  conductive pathway, as reflected by the steady-state levels of the clamping current ( $I_t$ ), skin conductance ( $G_t$ ), and the time course of  $I_t$  activation. The results compare the effects of two of  $\text{pH}_a$  values (8 and 4) at four different

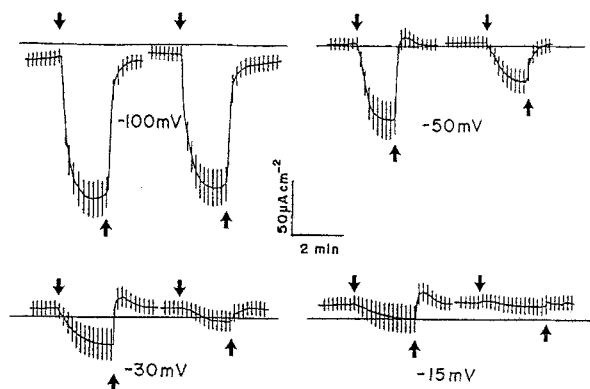


**Fig. 1.**  $I_t$  as a function of time for a representative experiment (of a group of 8 skins) performed in a single piece of tissue showing the effects of  $\text{pH}_a$  on the activation of the  $\text{Cl}^-$  conductive pathway. The skin was bathed on the inner side by NaCl Ringer. The four panels present similar sequences of two measurements each performed at the indicated clamping potential. The first measurement of each panel was carried out at  $\text{pH}_a = 8$  and the second, at  $\text{pH}_a = 4$ . For each measurement, activation of  $I_t$  was induced by a sudden rise of apical  $\text{Cl}^-$  concentration, obtained by replacing the apical solution, initially  $\text{K}_2\text{SO}_4$  57.5 mM, for a  $\text{KCl}$  115 mM solution at the same pH (downward arrows indicates  $\text{K}_2\text{SO}_4$  for  $\text{KCl}$  substitution). After being fully activated, the  $\text{Cl}^-$  pathway was deactivated by flushing the apical compartment with the initial bathing solution of  $\text{K}_2\text{SO}_4$  (upward arrows indicates  $\text{KCl}$  for  $\text{K}_2\text{SO}_4$  substitution). The vertical bars are deflections of  $I_t$  induced by  $V_t$  shifts of  $\pm 10$  mV.

levels of  $V_t$  ( $-100, -50, -30$  and  $-15$  mV). A representative experiment of a group of 8 tissues is shown in Fig. 1. Tissue bathing solutions are described in the legend of Fig. 1. Activation of the  $\text{Cl}^-$ -conductive pathway was induced by a sudden rise of  $[\text{Cl}^-]_a$ , while  $V_t$  was held at a preset level. It can be seen (Fig. 1) that the effect of a rise of  $[\text{Cl}^-]_a$  on the activation of  $G_{\text{Cl}}$  is markedly affected by  $\text{pH}_a$  as well as  $V_t$ . Thus, for  $V_t = -100$  mV the time course of  $I_t$  activation and the steady-state levels of  $I_t$  and  $G_t$  do not differ when experiments performed at  $\text{pH}_a = 8$  and  $\text{pH}_a = 4$  are compared. For higher  $V_t$  values ( $-50, -30$  and  $-15$  mV), in contrast, the level of activation (characterized by the steady-state values of  $I_t$  and  $G_t$ ) is smaller and the time course of  $I_t$  activation is longer in experiments performed at  $\text{pH}_a = 4$  as compared to experiments at  $\text{pH}_a = 8$ . These effects of apical solution acidification upon the activation of the  $\text{Cl}^-$ -conductive pathway are entirely reversible.

Acidification of the apical solution not only affects the process of activation of the  $\text{Cl}^-$  conductive pathway, as shown above, but it also influences the steady-state level of activation previously attained at a more alkaline pH (normally  $\text{pH}_a = 8$ ). This is shown for a representative experiment of a group of 6 skins in Fig. 2, where a skin clamped at  $-50$  mV had the  $\text{Cl}^-$ -conductive pathway activated by a sudden rise of  $[\text{Cl}^-]_a$ . With the  $\text{Cl}^-$ -conductive pathway fully activated, acidification of the apical solution from pH 8 to pH 4 led to a conspicuous

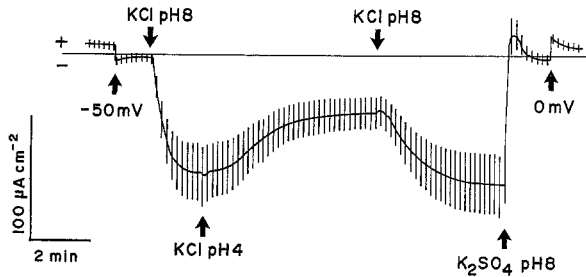


**Fig. 2.**  $I_t$  as a function of time for a representative experiment, of a group of 6 skins, showing the effect of  $\text{pH}_a$  on the steady-state level of activation of the  $\text{Cl}^-$  conductive pathway. The skin was bathed on the inner side by NaCl-Ringer, on the apical side by a solution of  $\text{K}_2\text{SO}_4$  57.5 mM at pH 8, and short-circuited. Subsequently  $V_t$  was clamped to  $-50$  mV and the  $\text{Cl}^-$  conductive pathway activated by replacing the apical solution by a KCl solution 115 mM at the same pH. When a steady state of activation was attained, the apical solution was replaced for approximately 6 min by a solution of KCl 115 mM at pH 4 and, subsequently, the apical solution was returned to pH 8. The vertical bars are deflections of  $I_t$  induced by  $V_t$  shifts of  $\pm 10$  mV.

inactivation of the  $\text{Cl}^-$ -conductive pathway that is characterized by a reduction of  $G_t$  and a shift of  $I_t$  to more positive levels. As shown in Fig. 2, this effect reverts completely when the apical solution is again returned to pH 8.

The results of experiments performed according to the protocol of Fig. 1 are summarized in Table 1 which shows mean steady-state values of  $I_t$  and  $G_r$  as well as the half times of  $I_t$  activation for two  $\text{pH}_a$  values (8 and 4) and four levels of  $V_t$  ( $-100$ ,  $-50$ ,  $-30$  and  $-15$  mV). From the present results it can be concluded that activation of the  $\text{Cl}^-$  conductive pathway is significantly affected by  $\text{pH}_a$  and  $V_r$ .

To determine the effects of apical solution acidification (in the  $\text{pH}_a$  range of 8 to 4) on  $I_t$  and  $G_t$  in the absence of apical  $\text{Cl}^-$  ions, experiments were performed having a  $\text{K}_2\text{SO}_4$  (57.5 mM) solution in the apical compartment and NaCl Ringer in the inner compartment. Table 2 shows that acidification of the apical solution from pH 8 to pH 4 leads to a small increase of  $I_t$  for all  $V_t$  values studied, except for  $V_t = -100$  mV, while  $G_t$  is not significantly affected by apical acidification at any clamping potential.

#### CHARACTERIZATION OF A VOLTAGE-DEPENDENT $\text{H}^+$ -GATED CONDUCTIVE PATHWAY

This study was carried out to analyze in more detail the effects of apical solution acidification upon  $I_t$  and  $G_r$ . The experiments were performed in the absence of apical  $\text{Cl}^-$  ions.

The results show the existence of a clear transition in the electrophysiological behavior of skins when  $\text{pH}_a$  is reduced to values below 4 and characterize the existence

of a voltage-dependent proton-gated conductance which is not related to the presence of  $\text{Cl}^-$  ions in the apical solution.

The experiments were performed in skins bathed on the apical surface by a solution of  $\text{K}_2\text{SO}_4$  (57.5 mM), on the inner surface by NaCl-Ringer and initially short-circuited. Acidification of the apical solution from pH 8 to pH 3 (Fig. 3, first run) and to pH 4 (Fig. 4, upper trace) were carried out, followed by a subsequent shift of  $V_t$  to  $-100$  mV. In the short-circuited condition, apical solution acidification to pH 4 or pH 3 causes a minor positive deflection of  $I_t$  which rapidly reaches a steady-state level. In most cases, as shown in Fig. 3, the increase of  $I_t$  is only transient.  $G_r$  on the other hand, is not affected by apical solution acidification at both pHs. A subsequent tissue hyperpolarization ( $V_t$  shift to  $-100$  mV) has a completely distinct outcome according to the apical pH, indicating the existence of a turning point between  $\text{pH}_a = 4$  and  $\text{pH}_a = 3$ . For  $\text{pH}_a = 4$  (as well as for  $\text{pH}_a$ s above 4, *not shown*), the skin responds to hyperpolarization ( $V_t = -100$  mV) are ohmic (Fig. 4), being characterized by a negative deflection of  $I_t$  and constancy of  $G_r$ . Subsequent return to the short-circuited condition and to  $\text{pH}_a = 8$  brings  $I_t$  to the initial control level. In contrast, at  $\text{pH}_a = 3$  (Fig. 3), skin hyperpolarization to  $-100$  mV causes an instantaneous ohmic response (similar to that seen at  $\text{pH}_a = 4$ , and characterized by a sharp negative deflection of  $I_t$ ) that is followed by a slow and pronounced sigmoidal increase of  $I_t$  which attains a stationary condition with a half-time of 43 sec ( $n = 8$  skins). This current response is accompanied by slow and marked increase of  $G_r$ . At  $\text{pH}_a = 3$ , a  $V_t$  shift from 0 mV to  $-100$  mV causes  $G_t$  to increase from  $0.94 \pm 0.08$  msec/cm<sup>2</sup> to  $3.6 \pm 0.22$  msec/cm<sup>2</sup> ( $P < 0.01$ ), and  $I_t$  to shift from  $55.0 \pm 3.7$  mA/cm<sup>2</sup> to  $-236.0 \pm 19.1$  mA/cm<sup>2</sup> ( $P < 0.01$ ). These changes of  $I_t$  and  $G_r$  which take place at  $\text{pH}_a = 3$  in response to skin hyperpolarization may reflect a slow activation of a voltage-dependent  $\text{H}^+$ -gated conductive pathway. A slow inactivation occurs when the skin is returned to the short-circuited condition (Fig. 3), indicating that the system behaves in a totally reversible way. The sequence in which tissue is hyperpolarized and the apical solution acidified is irrelevant for the activation of the voltage-dependent proton-gated conductance. Thus, if a skin initially bathed by an apical solution of  $\text{K}_2\text{SO}_4$  57.5 mM at  $\text{pH}_a = 8$  is clamped to  $-100$  mV, an ohmic response is observed. A subsequent acidification of the apical solution has a completely different outcome depending whether  $\text{pH}_a$  is shifted to a value above or below the turning point, which is somehow between  $\text{pH}_a = 4$  and  $\text{pH}_a = 3$ . Apical acidification to pH 3 caused a slow sigmoidal increase of  $I_t$  accompanied by a slow increase of  $G_t$  towards steady-state values, as shown in Fig. 3 (second run). In contrast, apical acidification to pH 4 (Fig. 4, lower trace) or pHs above 4 (*not shown*) causes no significant effect upon  $I_t$  or  $G_r$ . Finally, return to  $\text{pH}_a$

**Table 1.** Effects of  $\text{pH}_a$  and  $V_t$  upon the  $\text{Cl}^-$  conductive pathway

$V_t$ (mV)	$I_t$ ( $\mu\text{A cm}^{-2}$ )		$G_t$ ( $\text{mS cm}^{-2}$ )		$t_{1/2}$ (s)	
	$\text{pH}_a$ 8	$\text{pH}_a$ 4	$\text{pH}_a$ 8	$\text{pH}_a$ 4	$\text{pH}_a$ 8	$\text{pH}_a$ 4
-100	$-247.9 \pm 37.2$	$-235.1 \pm 35.3$ ns	$30.4 \pm 3.4$	$31.1 \pm 3.8$ ns	$18.2 \pm 3.8$	$14.9 \pm 1.9$ ns
-50	$-99.1 \pm 23.6$	$-48.3 \pm 12.3^*$	$27.7 \pm 5.0$	$18.6 \pm 2.8^*$	$19.3 \pm 1.3$	$33.1 \pm 1.2^{**}$
-30	$-36.0 \pm 13.4$	$-7.7 \pm 4.6^*$	$23.4 \pm 4.6$	$15.5 \pm 2.0^*$	$21.5 \pm 2.4$	$37.4 \pm 2.7^*$
-15	$-1.4 \pm 3.1$	$7.8 \pm 1.2^*$	$11.2 \pm 1.9$	$7.6 \pm 0.8^*$	$29.8 \pm 5.6$	$38.8 \pm 4.3^*$

Effects of  $\text{pH}_a$  and  $V_t$  on the steady-state levels of activation of the  $\text{Cl}^-$  conductive pathway, as indicated by the stationary values of  $I_t$  and  $T_p$ , and the time course of activation of the  $\text{Cl}^-$  conductive pathway, evaluated by the half-time of  $I_t$  activation ( $t_{1/2}$ ). The experiments were carried out according to the protocol described in the legend of Fig. 1. \* $P < 0.05$ , \*\* $P < 0.01$ ,  $n = 8$ .

**Table 2.** Effects of  $\text{pH}_a$  and  $V_t$  upon  $I_t$  and  $G_t$  in the absence of apical  $\text{Cl}^-$ 

$V_t$ (mV)	$I_t$ ( $\mu\text{A cm}^{-2}$ )		$G_t$ ( $\text{mS cm}^{-2}$ )	
	$\text{pH}_a$ 8	$\text{pH}_a$ 4	$\text{pH}_a$ 8	$\text{pH}_a$ 4
-100	$-36.9 \pm 2.6$	$-38.6 \pm 5.9$ ns	$9.8 \pm 0.9$	$11.9 \pm 1.3$ ns
-50	$-2.6 \pm 2.3$	$4.1 \pm 1.9^{**}$	$9.9 \pm 1.5$	$9.5 \pm 1.1$ ns
-30	$8.1 \pm 2.7$	$14.7 \pm 1.9^{**}$	$9.6 \pm 1.7$	$9.6 \pm 1.2$ ns
-15	$9.5 \pm 1.6$	$12.3 \pm 1.2^{**}$	$4.9 \pm 0.6$	$4.9 \pm 0.5$ ns
0	$27.4 \pm 7.7$	$40.5 \pm 5.6^*$	$8.6 \pm 1.0$	$9.2 \pm 1.1$ ns

Effects of  $\text{pH}_a$  and  $V_t$  on the steady-state levels of  $I_t$  and  $G_t$  in the absence of  $\text{Cl}^-$  ions in the apical solution. The skins were initially bathed on the inner side by NaCl-Ringer's and on the apical side by a solution of  $\text{K}_2\text{SO}_4$  57.5 mM at pH 8 and short-circuited.  $V_t$  was then shifted to the desired potential and, subsequently, the apical solution had its pH reduced to 4. \* $P < 0.05$ , \*\* $P < 0.01$ ,  $n = 8$ .

= 8, despite keeping the tissue hyperpolarized, deactivates the conductance,  $G_t$  and  $I_t$  returning to their previous levels (Fig. 3).

The striking similarity between the activation of the  $\text{Cl}^-$ -conductive pathway (Larsen & Rasmussen, 1982; Lacaz-Vieira & Procopio, 1988a; Larsen, 1991) and the activation of the voltage-dependent proton-gated pathway can be seen in Fig. 5, for a representative experiment, in which the voltage-dependent  $\text{Cl}^-$ -gated conductance was activated followed by activation of the voltage-dependent proton-gated conductance.

#### CURRENT-VOLTAGE CURVES OF THE VOLTAGE-DEPENDENT $\text{H}^+$ -GATED PATHWAY

##### Steady-State Measurements

Skins bathed on the apical side by a  $\text{K}_2\text{SO}_4$  solution (57.5 mM) and on the inner side by NaCl Ringer exhibit steady-state current-voltage curves that are highly dependent on the pH of the apical solution. In the  $\text{pH}_a$  range of 8 to 4, the steady-state current-voltage curves are linear, consistent with a preparation exhibiting a simple ohmic behavior. In contrast, experiments performed at  $\text{pH}_a = 3$

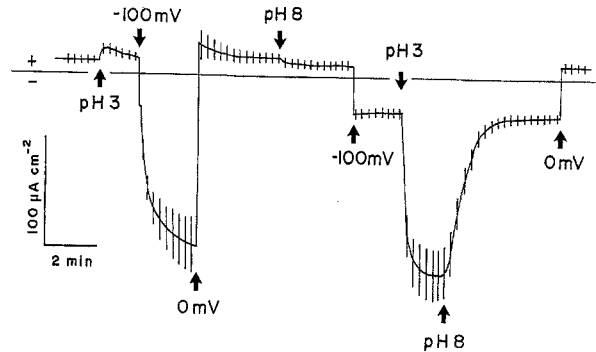


**Fig. 3.**  $I_t$  as a function of time for a representative experiment, of a group of 6 skins, showing the mutual effects  $\text{pH}_a$  (8 and 3) and tissue hyperpolarization to  $-100$  mV on the activation of a voltage-dependent  $\text{H}^+$ -gated conductance. The skin was bathed on the inner side by NaCl-Ringer and on the apical side by a solution of  $\text{K}_2\text{SO}_4$  57.5 mM. Initially, the apical solution had pH 8 and the preparation was short-circuited. Then  $\text{pH}_a$  and  $V_t$  were changed as indicated in the figure. The vertical bars are deflections of  $I_t$  induced by  $V_t$  shifts of  $\pm 10$  mV.

show a highly nonlinear dependence, with current flowing more easily in the outward direction. Fig. 6A illustrates a representative experiment of a group of 8 skins in which the steady-state  $I_t$ -vs- $V_t$ -relationship is depicted for a single skin at two  $\text{pH}_a$  values. At  $\text{pH}_a = 8$  the relationship is linear, while at  $\text{pH}_a = 3$  the dependence is markedly nonlinear. This highly nonlinear behavior observed at  $\text{pH}_a = 3$  is better illustrated for this group of skins in Fig. 6B, which shows mean  $G_t$  values increasing markedly in the negative range of clamping potentials, while at  $\text{pH}_a = 8$  the  $G_t \times V_t$  relationship is linear. These results show that the preparation exhibits a clear rectification when steady-state values are concerned. The time courses of  $I_t$  and  $G_t$  changes, induced by negative and positive clamping potentials, are shown for a representative experiment in Fig. 7.

##### “Instantaneous” $I_t$ vs. $V_t$ relationship

Determinations of the “instantaneous”  $I_t$  vs.  $V_t$  relationships (see Materials and Methods) were carried out at

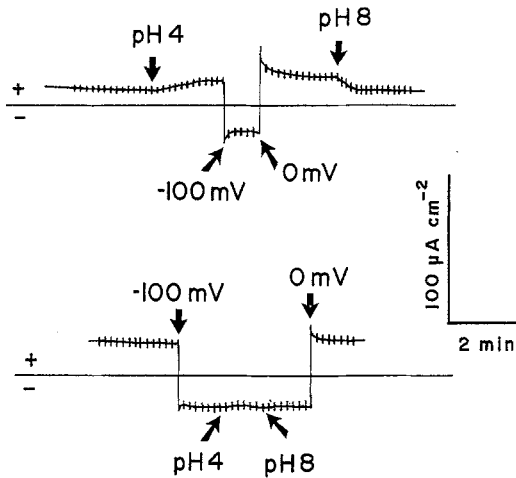


**Fig. 4.**  $I_t$  as a function of time for a representative experiment (of a group of 6 skins) showing the effects of  $\text{pH}_a$  (8 and 4) and skin hyperpolarization to  $-100$  mV upon  $I_t$  and  $G_t$ . The skin was bathed on the inner side by NaCl-Ringer and on the apical side by a solution of  $\text{K}_2\text{SO}_4$  57.5 mM. Initially,  $\text{pH}_a$  was set to 8 and the preparation short-circuited for both upper and lower traces. Then  $\text{pH}_a$  and  $V_t$  were changed as indicated in the figure. The vertical bars are deflections of  $I_t$  induced by  $V_t$  shifts of  $\pm 10$  mV.

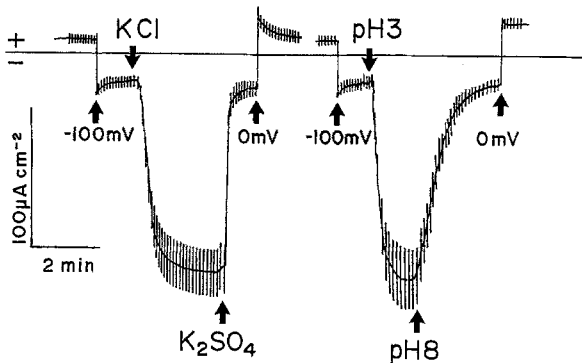


**Fig. 5.** A representative experiment performed in a single piece of skin in which the voltage-dependent  $\text{Cl}^-$ -gated conductance and the voltage-dependent proton-gated conductance are subsequently activated. The skin was bathed on the inner side by NaCl-Ringer and on the apical side by a solution of  $\text{K}_2\text{SO}_4$  (57.5 mM) with  $\text{pH}_a$  adjusted to 8. In the first run  $G_{\text{Cl}}$  was activated by shifting the clamping potential to  $-100$  mV and replacing the apical solution by a KCl solution at pH 8. Conductance inactivation was obtained by returning to a  $\text{K}_2\text{SO}_4$  solution on the apical side. In the second run the voltage-dependent proton-gated conductance was activated by shifting the clamping potential to  $-100$  mV and replacing the apical solution by a  $\text{K}_2\text{SO}_4$  solution at pH 3. Conductance inactivation was obtained by returning to a  $\text{K}_2\text{SO}_4$  solution at pH 8 on the apical side. Between the first and second runs there was an interval of approximately 6 min. The vertical bars are deflections of  $I_t$  induced by  $V_t$  shifts of  $\pm 10$  mV.

various  $\text{pH}_a$ s, clamping potentials (holding potentials) and levels of activation of the voltage-dependent proton-gated conductive pathway. A representative experiment (Fig. 8A) of a group of 6 skins shows the time course of

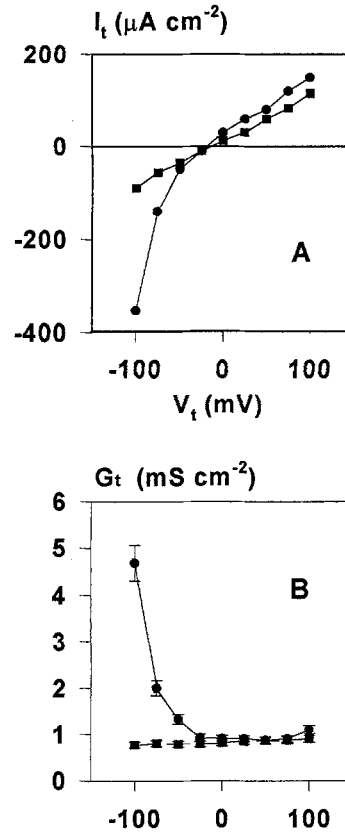


**Fig. 6.** (A) A representative experiment (of a group of 8 skins) showing steady-state current-voltage curves obtained at two  $\text{pH}_a$  values. Skins were bathed on the inner side by NaCl-Ringer and on the apical side by solutions of  $\text{K}_2\text{SO}_4$  (57.5 mM) with  $\text{pH}_a$  adjusted to 8 (squares) or to 3 (dots). (B) Mean values of steady-state conductance-voltage curves for the same group of skins at the same conditions of panel A.

$I_t$  and  $G_t$  activation and the instants data acquisition were carried out. Except for those measurements taken along the conductance deactivation period (c and d in Fig. 8A), the other determinations were performed when  $G_t$  and  $I_t$  had attained steady-state values. As the data acquisition intervals for the "instantaneous"  $I_t$  vs.  $V_t$  curves lasted 2 sec and the voltage pulses (100 msec each) were alternatively positive and negative, it can be assumed that the overall skin steady-state conditions (determined by the holding potential and  $\text{pH}_a$ ) prevailing just prior to the sequence of voltage pulses also hold during the acquisition period. Fig. 8B shows for the same experiment illustrated in Fig. 8A that, for all conditions tested, current and voltage are linearly related. The behavior depicted by this representative skin is very similar to the other 5 skins studied in this group. From these results, it can be concluded that the voltage-dependent proton-gated conductive pathway does not display any instantaneous rectifying property.

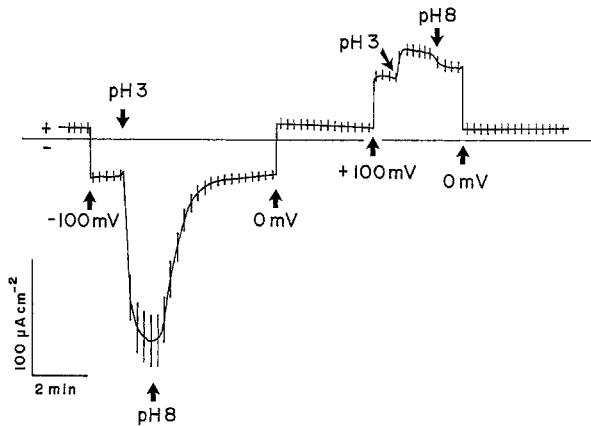


**Fig. 7.**  $I_t$  as a function of time for a representative experiment (of a group of 6 skins) showing the time course of activation of the voltage-dependent  $H^+$ -gated conductive pathway. The skin was initially short-circuited, bathed on the inner side by NaCl-Ringer and on the apical side by  $K_2SO_4$  57.5 mM at pH 8. Subsequently,  $V_t$  and  $pH_a$  were changed as indicated in the figure. The vertical bars are deflections of  $I_t$  induced by  $V_t$  shifts of  $\pm 10$  mV.

#### THE VOLTAGE-DEPENDENT $H^+$ -GATED CONDUCTANCE AND THE VOLTAGE-DEPENDENT $Cl^-$ -GATED CONDUCTANCE ARE RELATED TO TWO FUNCTIONALLY DISTINCT PATHWAYS

A marked similarity is observed between the time courses of activation of the voltage-dependent  $Cl^-$ -gated conductance and the voltage-dependent  $H^+$ -gated conductance (compare Fig. 3 and Fig. 5) and their steady-state and "instantaneous" current  $\times$  voltage and conductance  $\times$  voltage curves (compare Figs. 6, 7 and 8 with Fig. 3 in (Larsen, 1991)). To determine whether the conductive pathways activated in skins hyperpolarized to  $-100$  mV by a rise of apical  $Cl^-$  or apical proton concentration are functionally related experiments were carried out in a group of skins initially short-circuited, bathed on the apical side by  $K_2SO_4$  57.5 mM at  $pH_a = 8$ , and on the inner side by NaCl Ringer. Subsequently,  $V_t$  was clamped to  $-100$  mV and a few minutes later the apical solution was replaced by KCl 115 mM at  $pH_a = 8$ , ensuing a conspicuous activation of  $G_{Cl}$ . When this conductance was fully activated, and a steady state had been reached, replacement of the apical solution by a  $K_2SO_4$  solution at  $pH_a = 3$  led to a sharp reduction of  $I_t$  amplitude, followed by a rapid increase toward a new highly conductive state (Fig. 9). The significance of this finding is presented in the Discussion.

#### Discussion

The present study focuses on two closely related topics on ion conductance in toad skins: (i) the interaction of apical protons with the voltage-dependent  $Cl^-$ -activated

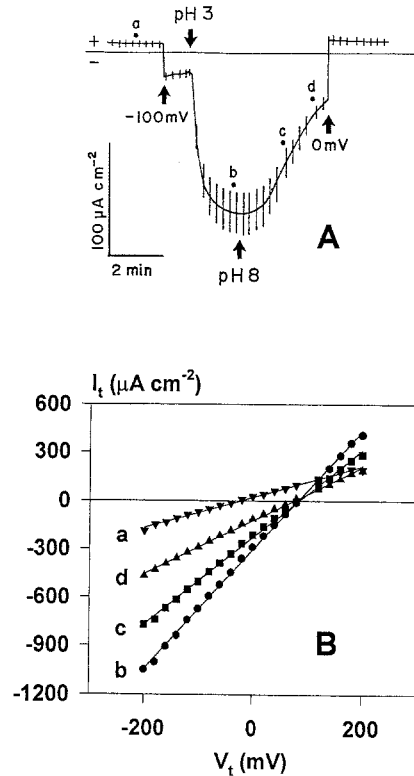


**Fig. 8.** (A)  $I_t$  as a function of time for a representative experiment showing activation of the voltage-dependent  $H^+$ -gated conductive pathway. The skin was initially short-circuited, bathed on the inner side by NaCl-Ringer and on the apical side by  $K_2SO_4$  57.5 mM at pH 8. Subsequently,  $V_t$  was clamped to  $-100$  mV and later the conductance activated by lowering  $pH_a$  to 3. Conductance deactivation was induced by returning  $pH_a$  to 8. The dots (a, b, c and d) mark the instants in which the instantaneous  $I_t \times V_t$  relationships were measured. The vertical bars are deflections of  $I_t$  induced by  $V_t$  shifts of  $\pm 10$  mV. (B) Instantaneous  $I_t \times V_t$  relationships obtained at instants marked by dots (a, b, c and d) in A. The straight lines are regression lines fitted to the data points.

conductance, and (ii) the description and characterization of a novel subject, a voltage-dependent  $H^+$ -activated conductance.

#### EFFECT OF APICAL PROTON CONCENTRATION ON THE ACTIVATION OF $G_{Cl}$

This project aimed to test the interaction of protons with the  $Cl^-$  channels, presumably located in the apical membrane of the MR cells of amphibian skins (Foskett & Ussing, 1986; Spring & Ussing, 1986; Larsen, Ussing & Spring, 1987; Larsen & Harvey, 1994) to evaluate the role of apical membrane fixed charges in the process of  $Cl^-$  channel activation.

The present study shows that increasing apical proton concentration (from pH 8 to pH 4) affects the process

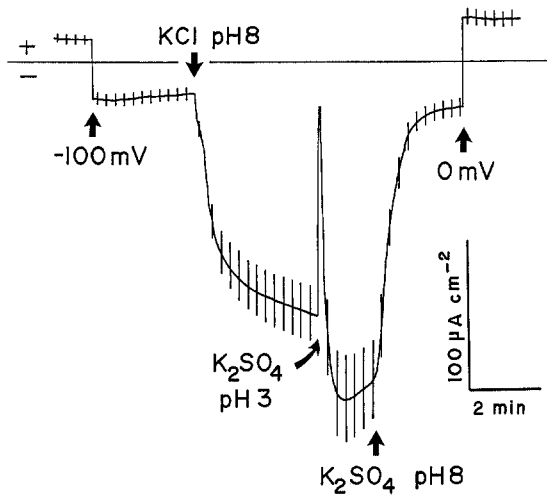


**Fig. 9.**  $I_t$  as a function of time for a representative experiment (of a group of 6 skins) showing that the conductance activated by hyperpolarized skins by apical  $\text{Cl}^-$  ions or by apical  $\text{H}^+$  ions refer indeed to two functionally distinct pathways. The skin bathed on the inner side by NaCl-Ringer and on the apical side by  $\text{K}_2\text{SO}_4$  57.5 mM at pH 8 was initially short-circuited. Subsequently,  $V_t$  was clamped to  $-100$  mV and later the apical solution was replaced by KCl 115 mM at pH 8, ensuring a conspicuous activation of  $G_{\text{Cl}}$ . When this conductance was fully activated, replacement of the apical solution by  $\text{K}_2\text{SO}_4$  at pH 3 leads to a sharp positive current deflection, compatible with the impermeability of the  $\text{Cl}^-$  pathways to  $\text{SO}_4^{2-}$ . Soon after, activation of the  $\text{H}^+$ -gated voltage-dependent conductive pathway takes place, characterized by a negative  $I_t$  deflection and increase of  $G_r$ .

of activation of the  $\text{Cl}^-$ -conductive pathway since it slows down the kinetics of  $I_t$  activation and reduces the steady-state values of  $G_t$  and  $I_t$  (Figs. 1 and 2; Table 1). The voltage dependence of the pH effect might indicate that the critical protonation sites of the  $\text{Cl}^-$  channels are not freely exposed to the apical solution but are located within the membrane electric field. The concentration of protons at these binding sites are expected to conform to a Boltzmann distribution. This interpretation permits one to understand the absence of any effect when apical solution acidification is carried out at a clamping potential of  $-100$  mV, while a conspicuous inhibition of  $G_{\text{Cl}}$  is observed when acidification is performed at  $-50$  mV (Fig. 1 and Table 1). It is also conceivable that changes in the membrane electric field causes conformational changes in the  $\text{Cl}^-$  channel protein, exposing the proton binding sites, which otherwise were occluded. An also coherent interpretation would be that titration of apical proton binding sites affects the gating of the voltage-dependent  $\text{Cl}^-$  channels, shifting the conductance-*vs.*-voltage curve to more negative clamping potentials, in a way similar to what was observed for the  $\text{Ca}^{2+}$ -dependent  $\text{K}^+$  channels in response to changes in the  $\text{Ca}^{2+}$  concentration in the *cis* side (Latorre, Vergara & Hidalgo, 1982). The absence of pH effect on tissue conductance at  $-100$  mV would mean that at this potential

the conductance-*vs.*-voltage curves, obtained at  $\text{pH}_a = 4$  and  $\text{pH}_a = 8$ , are in their plateau regions, where the conductance is no longer affected by the potential difference across the membrane. In consonance with this interpretation is the fact that the apical  $\text{Cl}^-$  channels of the MR cells in toad skin epithelium are modulated by c-AMP, the effect also being a displacement of the conductance-*vs.*-voltage curve to more positive clamping potentials (Willumsen, Vestergaard & Larsen, 1992).

The effects of apical proton concentration and clamping potential upon  $G_{\text{Cl}}$  might result from the protonation of sites which modulate the kinetics of activation of the apical  $\text{Cl}^-$  channels. The reduction in the steady-state values of  $G_t$  and  $I_t$  in response to apical solution acidification cannot result from a decrease of the single-channel conductance due to a reduction of the effective  $\text{Cl}^-$  concentration at the channel entrance since protonation of outward-facing negative charges would have a converse effect, increasing the  $\text{Cl}^-$  concentration in that region. Therefore, this effect and the observed increase in the time course of  $I_t$  activation, are strong indications that the protonation of membrane fixed charges affects the  $\text{Cl}^-$  channel itself. Additional evidence that the  $\text{Cl}^-$  channels are affected is that apical acidification from pH 8 to pH 4 in the absence of apical  $\text{Cl}^-$  ions does not effect tissue conductance for all tested clamping potentials (Table 2).

#### VOLTAGE-DEPENDENT PROTON-GATED CONDUCTANCE

In addition to the effects of apical protons on the activation of the  $\text{Cl}^-$  conductive pathway, the present study describes and characterizes the existence in the toad skin of a voltage-dependent proton-gated conductance. This conductance was characterized in the absence of apical  $\text{Cl}^-$  ions to rule out any contribution of  $\text{Cl}^-$  to the overall tissue conductance, since  $G_{\text{Cl}}$  is also activated by tissue hyperpolarization (Larsen & Rasmussen, 1982; Lacaz-Vieira & Procopio, 1988b).

Apical solution acidification carried out in  $\text{Cl}^-$ -free apical solution revealed a new and interesting aspect of the skin electrophysiological behavior, i.e., that tissue conductance in the absence of apical  $\text{Cl}^-$  ions can be importantly affected by the pH of the apical solution, the effect being markedly dependent on the clamping potential. Generally speaking, the effect of rising apical proton concentration can be conspicuous at negative clamping potentials, while at positive potentials changes in tissue conductance were never observed even for apical pHs as low as pH 3. In the negative range of clamping potentials, a turning point pH can be clearly seen. Thus, for a clamping potential of  $-100$  mV, the turning point is between pH 4 and pH 3, since apical acidification to pH 4 has no effect upon tissue conductance while apical acidification to pH 3 leads to a marked, slow and revers-



ible increase of tissue conductance (Fig. 3). Both a low apical pH and a negative clamping potential are needed to induce conductance activation. Meeting only one of these requisites is not enough to activate the conductive pathway (Fig. 3). This feature enables us to characterize the conductance as a voltage-dependent proton-gated conductance. The location of this conductance is so far uncertain. Nevertheless, due to the striking similitude between the voltage-dependent  $\text{Cl}^-$ -gated conductance (*see* Larsen, 1991 for review) and the voltage-dependent proton gated conductance (in (i) time course of activation, (ii) requirement for a negative clamping potential and the presence of a specific ion species in the apical solution for activation to occur, (iii) instantaneous ohmic behavior, and (iv) steady-state rectification), a tempting assumption would be to associate the voltage-dependent proton-gated conductance to the apical  $\text{Cl}^-$  channels of the mitochondria-rich cells, and consider sulfate as a charge carrier. It is known that the  $\text{Cl}^-$  channel of the MR cells when activated is poorly selective, behaving more properly as an anion channel (Harck & Larsen, 1986). Supporting the assumption that  $\text{SO}_4^{2-}$  is a charge carrier is the fact that sulfate, apparently as a monovalent species ( $\text{KSO}_4^-$  or  $\text{HSO}_4^-$ ), is permeable across the apical  $\text{Cl}^-$  channels, the ratio of the anion rate coefficients,  $k_{\text{Cl}^-} : k_{\text{SO}_4^{2-}}$  being 1:0.035 (Larsen & Simonsen, 1988). In our present case, however, due to the low apical pH, the specificity of the modifier site and/or the translocation site could have been altered, the channels no longer needing apical  $\text{Cl}^-$  for activation and the  $\text{SO}_4^{2-}$  permeability increasing. Interaction of protons with ion channels may drastically alter their behavior. Thus, in chick dorsal root ganglion cells, a proton-induced transformation of calcium channel, resulting in alterations of the gating and permeability properties, has been described (Konnerth, Lux & Morad, 1987; Davies, Lux & Morad, 1988). Also, in hypothalamic neurons of the rat, a proton-gated current increased as extracellular pH decreased, the maximum response occurring near pH 4. The properties of this proton-operated channel were similar to those of the voltage-gated  $\text{Na}^+$  channel rather than the  $\text{Ca}^{2+}$  channel (Ueno, Nakaye & Akaike, 1992) suggesting a modification of the  $\text{Na}^+$  channels. Porin, the channel-forming protein of the outer membrane of Gram-negative bacteria, shows a pH-induced change of channel size, switching occurring over a very narrow range of pH (Todt, Rocque & McGroarty, 1992). Ion-conducting channels formed in lipid bilayers by diphtheria toxin (Mindell et al., 1994a) and colicin N (Wilmsen, Pugsley & Pattus, 1990) are highly dependent on pH. These studies show that minor pH-induced changes in the molecule may lead to drastic changes of function. A direct influence of pH on the conformation of channel proteins is a possibility to explain our results. It is conceivable that, in our case, ion channels of the apical membrane could have been altered by the combined ac-

tion of low apical pH and membrane depolarization, leading to an increase of tissue conductance. Yet, it is known that ions are able to interact both with protein channels as well as with the lipid component of the membrane (Cai & Jordan, 1990). The pH dependence of tissue conductance could, in principle, result from a partial titration of the negative charges of membrane lipids (phosphates or carboxyl groups), which would alter the lipid packing of the apical membrane where the channels are incorporated. It is known that  $\text{H}^+$  is able to cause dramatic changes in lipid ordering when its concentration in solution reaches a threshold value (Ohki & Duax, 1986; Van Dijk et al., 1978). Recently, it has been shown that pH changes may also affect molecular packing of pure phosphatidylcholine bilayers (Massari et al., 1991).

A paracellular contribution to the voltage-dependent proton-gated conductance cannot be discarded. In skins of frog (*Rana esculenta* and *Rana temporaria*) (Fischbarg & Whittembury, 1978) and toad (*Bufo marinus*) (Gonzales et al., 1978) a critical apical pH value, lower than 2.5, was observed. Below this critical pH, the permeability of the paracellular pathway for sucrose increases and the total electrical resistance decreases reversibly. Our present results show that the critical apical pH value, or turning point, is highly dependent on the clamping potential. The voltage-dependence of the pH effect cannot be explained in terms of a rise of  $\text{H}^+$  ion concentration within the tight junctions leading to an increase in their permeability, since the polarity of the applied potential is opposite to that necessary for an effect to occur. This observation weakens the arguments in favor of a paracellular route for the voltage-dependent proton-gated conductance.

The results presented so far show a remarkable likeness between the voltage-dependent  $\text{Cl}^-$ -activated anion conductance (*see* Larsen, 1991 for review) and the voltage-dependent proton-activated conductance described in the present study (Fig. 5). The most important characteristics of these two conductances are that both: (i) rely on the presence of a certain type of ion in the apical solution ( $\text{Cl}^-$  or  $\text{H}^+$ , respectively); (ii) are activated by tissue hyperpolarization; (iii) present a slow time course of activation and deactivation; (iv) the steady-state  $I_t$ -vs.- $V_t$  relationship shows a marked rectification, with  $G_t$  increasing at the negative potential range, and (v) the instantaneous  $I_t$ -vs.- $V_t$  relationship is linear for all conditions studied. These similarities suggest that both conductances could indeed be related to a common pathway. The result shown in Fig. 9 is apparently conflicting with this interpretation, suggesting two independent systems, since the transient reduction of  $I_p$ , when the apical solution of KCl at pH 8 is replaced by a solution of  $\text{K}_2\text{SO}_4$  at pH 3 might indicate that  $G_{\text{Cl}^-}$  deactivates while the voltage-dependent proton-gated conductance is activated. However, a more plausible interpretation, in con-

sonance with the rest of the data, is that the lowering of apical pH could have altered the selectivity of the anion channel so that sulfate becomes a permeant ion. In this case, the transient reduction of  $I_t$  (Fig. 9) would be the result of the time taken for the new steady state to be reached.

In summary, the present study shows that increasing apical proton concentration impairs  $G_{Cl}$  activation in toad skin, this being a clearly voltage-dependent effect. In addition, we describe and characterize the existence of a voltage-dependent apical proton-gated conductance that might be closely related the voltage-dependent apical  $Cl^-$ -gated conductance well characterized in amphibian skins (for review see (Larsen, 1991; Lacaz-Vieira & Procopio, 1988a). These two conductances share very similar characteristics, as slow time courses of activation, highly nonlinear steady-state current-voltage curves and linear instantaneous current-voltage curves.

I greatly appreciate helpful discussions with Antonio Carlos Cassola and Erik Hviid Larsen. This project was supported by grants 94/0300-1 from Fundação de Amparo à Pesquisa do Estado de São Paulo, and 521869/94-3 NV from Conselho Nacional de Desenvolvimento Científico e Tecnológico, Brazil.

## References

- Apell, H.J., Bamberg, E., Läuger, P. 1979. Effects of surface charge on the conductance of the gramicidin channel. *Biochim. Biophys. Acta* **562**:369–378
- Behrens, M.I., Oberhauser, A., Bezaniilla, F., Latorre, R. 1989. Batrachotoxin-modified sodium channels from squid optic nerve in planar bilayers. *J. Gen. Physiol.* **93**:23–41
- Bruus, K., Kristensen, P., Larsen, E.H. 1976. Pathways for chloride and sodium transport across toad skin. *Acta Physiol. Scand.* **97**:31–47
- Cai, M., Jordan, P.S. 1990. How does vestibule charge affect ion conduction and toxin binding in sodium channel? *Biophys. J.* **57**:883–891
- Castro, J.A., Sesso, A., Lacaz-Vieira, F. 1993. Deposition of  $BaSO_4$  in the tight junctions of amphibian epithelia causes their opening; apical  $Ca^{2+}$  reverses this effect. *J. Membrane Biol.* **134**:15–29
- Chang, D., Kushman, N.L., Dawson, D.C. 1991. Intracellular pH regulates basolateral  $K^+$  and  $Cl^-$  conductances in colonic epithelial cells by modulating  $Ca^{2+}$  activation. *J. Gen. Physiol.* **98**:183–196
- Cuppoletti, J., Baker, A.M., Malinowska, D.H. 1993.  $Cl^-$  channels of the gastric parietal cell that are active at low pH. *Am. J. Physiol.* **264**:C1609–C1618
- Cuthbert, A.W., Painter, E. 1968. The effect of theophylline on chloride permeability and active chloride transport in various epithelia. *J. Pharm. Pharmacol.* **20**:492–495
- Davies, N.W., Lux, H.D., Morad, M. 1988. Site and mechanism of activation of proton-induced sodium current in chick dorsal root ganglion neurones. *J. Physiol.* **400**:159–187
- De Wolf, I., Van Driessche, W., Nagel, W. 1989. Forskolol activates gated  $Cl^-$  channels in frog skin. *Am. J. Physiol.* **256**:C1239
- Deutsch, C., Lee, S.C. 1989. Modulation of  $K^+$  currents in human lymphocytes by pH. *J. Physiol.* **413**:399–413
- Fischbarg, J., Whittembury, G. 1978. The effect of external pH on osmotic permeability, ion and fluid transport across isolated frog skin. *J. Physiol.* **275**:403–417
- Foskett, J.K., Ussing, H.H. 1986. Localization of chloride conductance to mitochondria-rich cells in frog skin epithelium. *J. Membrane Biol.* **91**:251–258
- Gogelein, H. 1989. Chloride channels in epithelia. *Biochim. Biophys. Acta* **947**:521–547
- Gonzales, E., Kirchhausen, T., Linares, H., Whittembury, G. 1978. Observations on the action of urea and other substances in opening the paracellular pathway in amphibian skins. In: How Organisms Regulate their Internal and External Environment. L. Bolis, S. Maddrell, K. Schmidt-Nielsen, editors. pp. 43–52. Cambridge University Press, Cambridge
- Green, W.N., Andersen, O.S. 1991. Surface charges and ion channel function. *Annu. Rev. Physiol.* **53**:341–359
- Harck, A.F., Larsen, E.H. 1986. Concentration dependence of halide fluxes and selectivity of the anion pathway in toad skin. *Acta Physiol. Scand.* **128**:289–304
- Hille, B. 1968. Charges and potentials at the nerve surface. Divalent ions and pH. *J. Gen. Physiol.* **51**:221–236
- Hille, B. 1992. Ionic Channels of Excitable Membranes. Sinauer Associates, Sunderland, MA
- Jordan, P.C. 1993. Interactions of ions with membrane proteins. In: Thermodynamic of Membrane Receptors and Channels. M.B. Jackson, editor. pp. 27–80. CRC Press, Boca Raton
- Katz, U., Larsen, E.H. 1984. Chloride transport in toad skin (*Bufo viridis*). The effect of salt adaptation. *J. Exp. Biol.* **109**:353–371
- Katz, U., Van Driessche, W. 1987. Effect of theophylline on the apical sodium and chloride permeabilities of amphibian skin. *J. Physiol.* **397**:223–236
- Klaerke, D.A., Wiener, H., Zeuthen, T., Jorgensen, P.L. 1993.  $Ca^{2+}$  activation and pH dependence of a maxi  $K^+$  channel from rabbit distal colon epithelium. *J. Membrane Biol.* **136**:9–21
- Konnerth, A., Lux, H.D., Morad, M. 1987. Proton-induced transformation of calcium channel in chick dorsal root ganglion cells. *J. Physiol.* **386**:603–633
- Kristensen, P. 1982. Chloride transport in frog skin. In: Chloride transport in biological membranes. J.A. Zadunaisky, editor. pp. 310–332. Academic, New York
- Kristensen, P. 1983. Exchange diffusion, electrodiffusion and rectification in the chloride transport pathways of frog skin. *J. Membrane Biol.* **72**:141–151
- Kristensen, P., Larsen, E.H. 1978. Relation between chloride exchange diffusion and a conductive chloride pathway across the isolated skin of the toad (*Bufo bufo*). *Acta Physiol. Scand.* **102**:22–34
- Kuwahara, M., Ishibashi, K., Krapf, R., Rector Jr., F.C., Berry, C.A. 1989. Effect of lumen pH on cell pH and cell potential in rabbit proximal tubules. *Am. J. Physiol.* **256**:F1075–F1083
- Lacaz-Vieira, F. 1986. Sodium flux in the apical membrane of the toad skin: aspects of its regulation and the importance of the ionic strength of the outer solution upon the reversibility of amiloride inhibition. *J. Membrane Biol.* **92**:27–36, 1986.
- Lacaz-Vieira, F., Procopio, J. 1988a. Chloride transport in amphibian skin: A review. *Brazilian J. Med. Biol. Res.* **21**:1119–1128
- Lacaz-Vieira, F., Procopio, J. 1988b. Comparative roles of voltage and  $Cl^-$  ions upon activation of a  $Cl^-$  conductive pathway in toad skin. *Pfluegers Arch.* **412**:634–640
- Larsen, E.H. 1982. Chloride Current Rectification in Toad Skin Epithelium. In: Chloride Transport in Biological Membranes. J. Zadunaisky, editor. pp. 333–364. Academic, New York
- Larsen, E.H. 1991. Chloride transport by high-resistance heterocellular epithelia. *Physiol. Rev.* **71**:235–283
- Larsen, E.H., Harvey, B.J. 1994. Chloride currents of single mitochondria-rich cells of toad skin epithelium. *J. Physiol.* **478**:7–15
- Larsen, E.H., Kristensen, P. 1978. Properties of a conductive cellular

- chloride pathway in the skin of the toad (*Bufo bufo*). *Acta Physiol. Scand.* **102**:1–21
- Larsen, E.H., Rasmussen, B.E. 1982. Chloride channels in toad skin. *Phil. Trans. R. Soc. Lond. B.* **299**:413–434
- Larsen, E.H., Rasmussen, B.E. 1983. Membrane potential plays a dual role for chloride transport across toad skin. *Biochim. Biophys. Acta* **728**:455–459
- Larsen, E.H., Rasmussen, B.E. 1985. A mathematical model of amphibian skin epithelium with two types of transporting cellular units. *Pfluegers Arch.* **405** (Suppl. 1):S50–S58
- Larsen, E.H., Simonsen, K. 1988. Sulfate transport in toad skin: evidence for mitochondria-rich cell pathways in common with halide ions. *Comp. Biochem. Physiol. A.* **90**:709–714
- Larsen, E.H., Ussing, H.H., Spring, K.R. 1987. Ion transport by mitochondria-rich cells in toad skin. *J. Membrane Biol.* **99**:25–40
- Latorre, R., Labarca, P., Naranjo, D. 1992. Surface charge effects on ion conductance in ion channels. *Methods Enzymol.* **207**:471–501
- Latorre, R., Vergara, C., Hidalgo, C. 1982. Reconstitution in planar lipid bilayers of a  $\text{Ca}^{2+}$ -dependent  $\text{K}^+$  channel from transverse tubule membranes isolated from rabbit skeletal muscle. *Proc. Nat. Acad. Sci. USA* **79**:805–809
- MacInnes, D.A. 1961. The principles of electrochemistry. Dover Publications, New York
- Mandel, L.J. 1975. Actions of external hypotonic urea, ADH, and theophylline on transcellular and extracellular solute permeability in frog skin. *J. Gen. Physiol.* **55**:599–615
- Massari, S., Folena, E., Ambrosin, V., Schiavo, G., Colonna, R. 1991. pH dependent lipid packing, membrane permeability and fusion in phosphatidylcholine vesicles. *Biochim. Biophys. Acta* **1067**:131–138
- Mindell, J.A., Silverman, J.A., Collier, R.J., Finkelstein, A. 1994a. Structure-function relationships in diphtheria toxin channels: II. A residue responsible for the channel's dependence on *trans* pH. *J. Membrane Biol.* **137**:29–44
- Mindell, J.A., Silverman, J.A., Collier, R.J., Finkelstein, A. 1994b. Structure-function relationships in diphtheria toxin channels: III. Residues which affect the *cis* pH dependence of channel conductance. *J. Membrane Biol.* **137**:45–57
- Neter, J., Wasserman, W. 1974. Applied linear statistical models. Richard D. Irwin, Homewood, IL
- Ohki, S., Duax, J. 1986. Effects of cations and polycations on the aggregation and fusion of phosphatidylserine membranes. *Biochim. Biophys. Acta* **861**:177–186
- Pietrobon, D., Prod'hom, B., Hess, P. 1989. Interaction of protons with single open L-type calcium channels. pH dependence of proton-induced current fluctuations with  $\text{Cs}^+$ ,  $\text{K}^+$ , and  $\text{Na}^+$  as permeant ions. *J. Gen. Physiol.* **94**:1–21
- Procopio, J., Lacaz-Vieira, F. 1990. Roles of external and cellular  $\text{Cl}^-$  ions on the activation of an apical electrodiffusional  $\text{Cl}^-$  pathway in toad skin. *J. Membrane Biol.* **117**:57–67
- Prod'hom, B., Pietrobon, D., Hess, P. 1989. Interactions of protons with single open L-type calcium channels. Location of protonation site and dependence of proton-induced current fluctuations on concentration and species of permeant ion. *J. Gen. Physiol.* **94**:23–42
- Pusch, M., Jentsch, T.J. 1994. Molecular physiology of voltage-gated chloride channels. *Physiol. Rev.* **74**:813–827
- Recio-Pinto, E., Thornhill, W.B., Duch, D.S., Levinson, S.R., Urban, B.W. 1990. Neuraminidase treatment modifies the function of electroplax sodium channels in planar lipid bilayers. *Neuron* **5**:675–684
- Rousseau, E., Pinkos, J. 1990. pH modulates conducting and gating behaviour of single calcium release channels. *Pfluegers Arch.* **415**:645–647
- Sherry, A.M., Cuppoletti, J., Malinowska, D.H. 1994. Differential acidic pH sensitivity of delta F508 CFTR  $\text{Cl}^-$  channel activity in lipid bilayers. *Am. J. Physiol.* **266**:C870–C875
- Spring, K.R., Ussing, H.H. 1986. The volume of mitochondria-rich cells of frog skin epithelium. *J. Membrane Biol.* **92**:21–26
- Suzuki, M., Takahashi, K., Ikeda, M., Hayakawa, H., Ogawa, A., Kawaguchi, Y., Sakai, O. 1994. Cloning of a pH-sensitive  $\text{K}^+$  channel possessing two transmembrane segments. *Nature* **367**:642–645
- Tang, C.M., Dichter, M., Morad, M. 1990. Modulation of the N-methyl-D-aspartate channel by extracellular  $\text{H}^+$ . *Proc. Natl. Acad. Sci. USA* **87**:6445–6449
- Todt, J.C., McGroarty, E.J. 1992. Involvement of histidine-21 in the pH-induced switch in porin channel size. *Biochemistry* **31**:10479–10482
- Todt, J.C., Rocque, W.J., McGroarty, E.J. 1992. Effects of pH on bacterial porin function. *Biochemistry* **31**:10471–10478
- Ueno, S., Nakaye, T., Akaike, N. 1992. Proton-induced sodium current in freshly dissociated hypothalamic neurones of the rat. *J. Physiol.* **447**:309–327
- Van Dijk, P.V.M., De Ckruif, B., Verkleij, A.J., Van Deenen, L.L.M., De Gier, J. 1978. Comparative studies on the effect of pH and  $\text{Ca}^{2+}$  on bilayers of various negatively charged phospholipids and their mixtures with phosphatidylcholine. *Biochim. Biophys. Acta* **557**:62–78
- Willmsen, N.J., Vestergaard, L., Larsen, E.H. 1992. Cyclic AMP- and b-agonist-activated chloride conductance of a toad skin epithelium. *J. Physiol.* **449**:641–653
- Wilmsen, H.U., Pugsley, A.P., Pattus, F. 1990. Colicin N forms voltage- and pH-dependent channels in planar lipid bilayer membranes. *Eur. Biophys. J.* **18**:149–158